



## Sensitivity of the magnetization curves of different austenitic stainless tube and pipe steels to mechanical fatigue

M. Niffenegger\*, H.J. Leber

Paul Scherrer Institut, Structural Integrity Group, Nuclear Energy and Safety Department, 5232 Villigen PSI, Switzerland

### ARTICLE INFO

#### Article history:

Received 5 September 2007

Accepted 10 March 2008

#### PACS:

85.80.Jm

81.40.Cd

81.40.Np

81.70.Ex

81.30.Kf

78.66.Bz

75.60.Ej

### ABSTRACT

In meta-stable austenitic stainless steels, fatigue is accompanied by a partial strain-induced transformation of paramagnetic austenite to ferromagnetic martensite [G.B. Olsen, M. Cohen, Kinetics of strain induced martensite nucleation, Metall. Trans. 6 (1975) 791–795]. The associated changes of magnetic properties as the eddy current impedance, magnetic permeability or the remanence field may serve as an indication for the degree of fatigue and therefore the remaining lifetime of a component, even though the exact causal relationship between martensite formation and fatigue is not fully understood. However, measuring these properties by magnetic methods may be limited by the low affinity for strain-induced martensite formation. Thus other methods have to be found which are able to detect very small changes of ferromagnetic contents. With this aim the influence of cyclic strain loading on the magnetization curves of the austenitic stainless tube and pipe steels TP 321, 347, 304L and 316L is analysed in the present paper. The measured characteristic magnetic properties, which are the saturation magnetization, residual magnetization, coercive field and the field dependent permeability (AC-magnetization), are sensitive to fatigue and the corresponding material changes (martensitic transformation). In particular, the AC-magnetization was found to be very sensitive to small changes of the amount of strain induced martensite and therefore also to the degree of fatigue. Hence we conclude that applying magnetic minor loops are promising for the non-destructive evaluation of fatigue in austenitic stainless steel, even if a very small amount of strain induced martensite is formed.

© 2008 Elsevier B.V. All rights reserved.

### 1. Introduction

Lifetime extension of nuclear power plants (NPP) requires the assurance of safe operation by appropriate safety assessment tools. Therefore, the early detection of possible material degradation prior to crack initiation of safety-relevant components, e.g. pipes in the primary loop of NPPs, is becoming more important.

Among several non-destructive testing techniques, conventional methods (e.g. ultra sonic and eddy current techniques) are widely-used to detect and size cracks. More advanced magnetic methods aiming for the detection of material degradation in the pre-cracked state are very promising; however, they are still under investigation.

Some of these magnetic methods are based on measuring strain-induced martensite fractions formed in meta-stable austenitic stainless steels (ASS) since fatigue of ASS is accompanied by a transformation of the paramagnetic face centred cubic phase ( $\gamma$ -fcc) into body centred tetragonal martensitic phase ( $\alpha'$ -bct) which is ferromagnetic [1–3]. The corresponding changes of magnetic

properties can be detected by measuring the eddy current impedance, the magnetic permeability and the remanence field. These methods have been extensively investigated by several research groups in the last decade [5–13]. It was shown that in meta-stable ASS  $\alpha'$ -formation can be used as an indication of the fatigue state, if the conditions listed below are fulfilled [4]:

- The affinity for the martensitic transformation has to be sufficiently high to allow the detection of the formed phase.
- Beside the chemical composition of the material, also its degree of cold-working and the final heat treating condition must be known.
- Knowledge of the loading conditions, i.e. strain amplitude, load mode and operating temperature is needed.

These conditions could in principle be fulfilled by generating specific calibration curves (reference curves) of the material under investigation. Furthermore, the operating conditions are known in most cases. However, as shown below, the high quality stainless steels installed in NPPs often exhibit very low affinity to form strain-induced martensite under typical operating conditions. It was also shown, that while magnetic changes can still be observed under laboratory conditions, the signal to noise ratio might be too

\* Corresponding author. Tel.: +41 56 310 2686; fax: +41 56 310 2199.

E-mail address: [Markus.Niffenegger@psi.ch](mailto:Markus.Niffenegger@psi.ch) (M. Niffenegger).

URL: <http://www.psi.ch> (M. Niffenegger).

bad for field applications. Hence magnetic methods which are even more sensitive to the magnetic changes than the ones mentioned above are demanded.

Seeking for such sensitive methods, we analysed the magnetic behaviour of several austenitic stainless tube and pipe steels (TP 321, 347, 304L and 316L), which are frequently used in primary loops of NNPs, by measuring their magnetization curves.

## 2. Investigated materials

Two types of materials are frequently used in primary loops of NNPs, namely ferritic steels, e.g. for the reactor pressure vessel, and austenitic stainless steel (ASS) for the piping of cooling systems. In this paper we concentrate on the properties of austenitic stainless tube and pipe (TP) steel.

ASS having a face centred cubic lattice ( $\gamma$ -phase), called austenite, may undergo a partial transformation to body centred cubic ( $\alpha'$ -phase) martensite, which is slightly distorted to a tetragonal shape dependent on the carbon content. Whereas the  $\gamma$ -phase exhibits paramagnetic properties the  $\alpha'$ -phase is ferromagnetic. Such transformations are driven by thermodynamic forces and/or by mechanical deformation. If the  $\alpha'$ -phase is formed by deformation, it is called strain-induced martensite. The strain-induced  $\alpha'$  is the target of our investigation. Since its formed amount is associated with the accumulated plastic strain and dislocation density, it can be used as an indication of the fatigue state. The measurability of  $\alpha'$  by magnetic methods is based on the properties mentioned above.

The investigated materials and their chemical compositions are summarized in Table 1. Three groups of ASS are distinguished in Table 1. The non-stabilized low-carbon steels TP 304L and TP 316L, the Ti-stabilized TP 321 and the Nb-stabilized TP 347 (L stands for low carbon, in view of the chemical composition, the products labelled with TP corresponds to the label AISI of ASME). These materials, used for primary cooling circuits in nuclear power plants (NPPs), possess high austenite stability or low affinity to strain-induced martensite formation due to their high metallurgical quality level.

All the investigated pipes were manufactured according to ASME SA-312/SA-312M and fulfil the requirements for the use in primary circuits of NPPs. Standard cylindrical fatigue specimens according to ASTM E 606 were cut from the pipes, all having a diameter of 219 mm, whereas their axis is parallel to that of the pipe. After fatiguing the specimens up to a certain usage factor  $D$ , a small ( $3 \times 3 \times 4$  mm) material probe was taken from the middle of the specimens for the magnetic measurements.  $D$  is defined by the ratio  $N/N_f$  with  $N$  being the number of applied strain cycles of certain amplitude and  $N_f$  is the number of cycles to crack detection, determined in fatigue tests by a 5% drop of the applied force. The following commercial tube and pipe materials have been investigated:

TP 304L (DIN 1.4306, X2CrNi19-11), wall thickness 23 mm,  
 TP 316L (DIN 1.4404, X2CrNiMo17-12-2), wall thickness 23 mm  
 TP 321 (DIN 1.4541, X6CrNiTi18-10), wall thickness 23 mm  
 TP 347 (DIN 1.4550, X6CrNiNb18-10), wall thickness 15.87 mm

## 3. Affinity for strain induced martensite formation

In general, martensite may appear either in lath, plate (twinned) or mixed shape, depending on temperature, chemical composition and applied load. However, in the materials discussed in this paper,  $\alpha'$  nucleates at the intersection of deformation bands. In addition to the morphology of the formed  $\alpha'$ , also the amount of  $\alpha'$  depends strongly on the chemical composition and production process, e.g. degree of cold-work, of the steel product. This is shown in Fig. 1 where the fraction of  $\alpha'$ , evaluated by means of magnetic NDT methods and neutron diffraction and by means of magnetic methods, versus the number of load cycles for different austenitic stainless steels is plotted. The increase of  $\alpha'$  in Fig. 1 is valid for a strain amplitude  $\Delta\epsilon_t/2 = 0.3\%$ . Note that each data point plotted in Fig. 1 corresponds to a particular specimen. Therefore the scatter of the material properties is already included in the results and is leading to a relatively large scatter in the  $\alpha'$ -content, especially for TP 321. In general it turned out that all the TP products exhibit a very low affinity for strain induced martensite formation. Nevertheless, in a well defined laboratory environment even this small amount of  $\alpha'$  can be measured by the mentioned magnetic NDT techniques, but their field application for these steel products seems to be difficult. As shown in Fig. 1, most  $\alpha'$  was formed in the Ti-stabilized TP 321, whereas the non-stabilized TP 304L and TP316L showed lowest affinity for  $\alpha'$ -formation. This is in accordance to the role of C which stabilizes the  $\gamma$ -phase, provided it is in solid solution. In the stabilized grades however the whole amount of C is expected to be precipitated in the carbonitrides of Ti or Nb, respectively.

Since different steels may exhibit different softening/hardening behaviour during fatigue and therefore pass a different path in the stress space, they may also differ in their accumulated plastic strain  $\epsilon_p^{acc} = \sum_{i=1}^N \Delta\epsilon_p^i$ , which is the sum of the plastic strain increments  $\Delta\epsilon_p$  taken over all  $N$  applied load cycles. Hence it makes sense to plot the amount of  $\alpha'$  versus the accumulated plastic

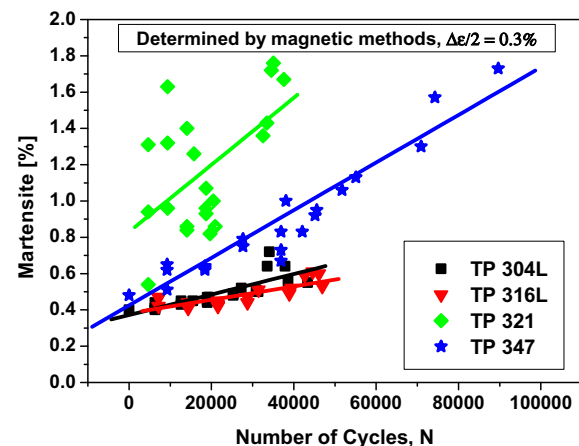


Fig. 1. Fraction of martensite vs. number of strain cycles determined with a permeability measurement. The specimens were fatigued at room temperature with a total strain amplitude of  $\Delta\epsilon_t/2 = 0.3\%$ .

Table 1

Chemical composition of the investigated materials taken from different original tube materials

TP	C	Si	Mn	P	S	Cr	Mo	Ni	Co	Cu	N	Nb	Ti
304L	0.029	0.20	1.77	0.020	0.004	19.0	0.122	10.35	0.034	0.186	0.0748	0.002	0.002
316L	0.021	0.26	1.69	0.033	0.003	17.5	2.15	11.14	0.093	0.273	0.0601	0.012	0.003
321	0.060	0.18	1.88	0.03	0.004	17.9	0.234	10.13	0.109	0.223	0.0107	0.015	<i>0.431</i>
347	0.055	0.27	1.74	0.023	0.006	17.9	0.351	10.48	0.102	0.225	0.0266	0.717	0.003

Values of the chemical contents are given in wt%. Stabilizing elements are italicized.

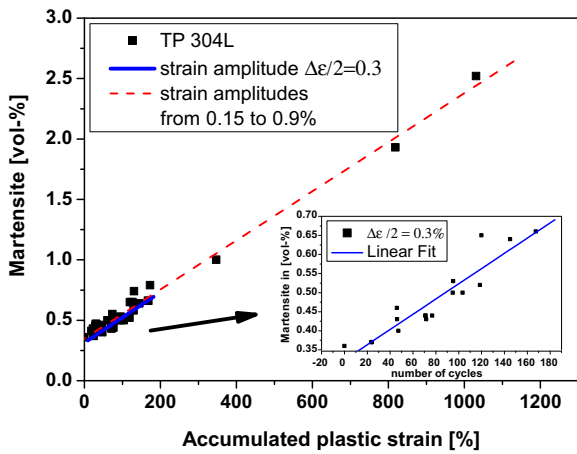


Fig. 2. Martensite fraction vs. accumulated plastic strain for TP 304L, resulting from fatigue tests with strain amplitudes ranging from 0.15 to 0.9%. A linear dependence is observed.

strain. In Fig. 2 the fraction of martensite, versus the accumulated plastic strain for TP 304L is plotted. A linear dependence of  $\alpha'$  on the accumulated plastic strain was found in the investigated strain range (total strain) between  $\Delta\epsilon_t/2 = 0.15$  and  $\Delta\epsilon_t/2 = 0.9\%$ , shown by the linear fit (red curve) of the experimental data. Whereas the red curve fits the results from different strain amplitudes, the blue curve represents the results for  $\Delta\epsilon_t/2 = 0.3\%$  only. We stress that the measured  $\alpha'$ -contents are averaged bulk values and that the local concentration of  $\alpha'$  may be higher. It is also worth mentioning that the magnetic NDT-methods (based on eddy current impedance, permeability and remanence field) were calibrated with a set of samples whose exact amount of  $\alpha'$  was preliminary determined by neutron powder diffraction at the neutron spallation source SINQ at the Paul Scherrer Institut, Switzerland (PSI) [14].

#### 4. DC-magnetization loops of TP 321, 347, 304L and TP 316L

For measuring the magnetization curves we used a Physical Properties Measuring System (PPMS) from Quantum Design, San Diego, CA. This apparatus allows measuring the magnetization of a vibrating sample in a magnetic field (Vibrating Sample Method, VSM). The high sensitivity of the PPMS is reached by detecting the induction of the moving and magnetized sample with a SQUID (Superconducting Interference Device). The measurements were performed in DC and AC mode.

In DC-mode an external magnetic field is increased and decreased up/down to certain field strength, in order to magnetize the sample. The resulting magnetization loop yields the saturation magnetization  $M_s$ , remanent magnetization  $M_R$ , coercive field  $M_C$  and the field dependent permeability of the tested material. A further property, the hysteresis heat  $I_{M_{DC}}$  was calculated by integrating the magnetization loop. All these characteristic properties are sensitive to fatigue and the corresponding material changes (martensite formation). Fig. 3 illustrates the magnetization loops with the characteristic magnetic properties of two samples, both made from bar stock material AISI 321, but containing different amount of martensite. Note that this material differs from the tube and pipe material TP 321, since it shows a much higher affinity for martensite formation. The magnetic loop for the bar stock material AISI 321 is shown in Fig. 3 in contrast to the TP material analysed in this paper.

The magnetization loops of material samples in different fatigue states were measured in the DC-mode of the PPMS. During a magnetization loop the magnetic field  $H$  was increased from  $-3000$  Oe up to  $+3000$  Oe and again back to  $-3000$  Oe, whereas the magnetization  $M$  was measured. The DC-magnetization loops for all the

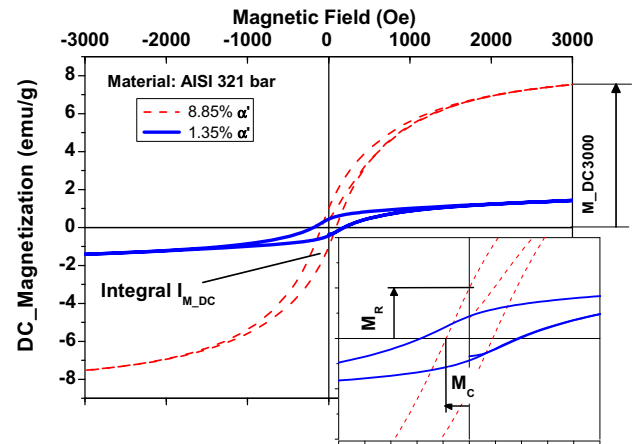


Fig. 3. DC-Magnetization loops and the corresponding characteristic properties for two samples made from bar stock AISI 321 with different contents of martensite.

investigated materials are shown in Figs. 4–7. In these figures the magnetization is plotted in electromagnetic units per gram (emu/g) versus the applied magnetic field for different usage factors indicated in the plot with  $D$ . As shown in the figures, no saturation magnetization was achieved for the applied field strength. Note that each curve corresponds to a different specimen.

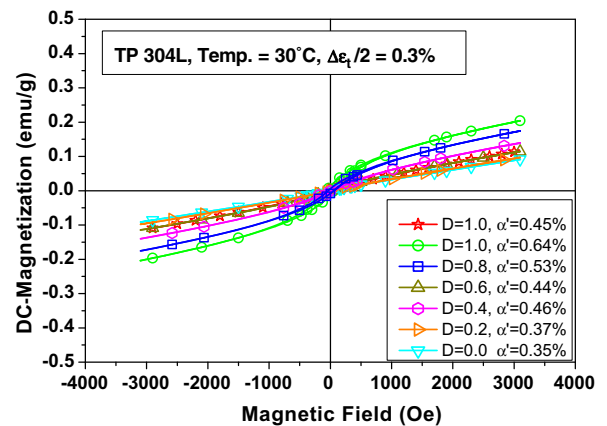


Fig. 4. Magnetization loop for TP 304L, cycled up to different usage factors  $D$ .

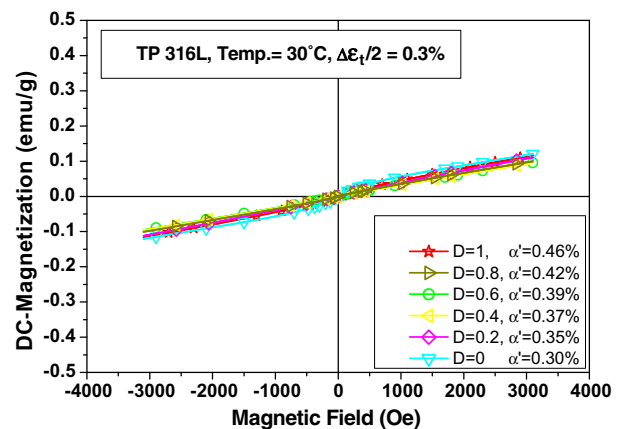


Fig. 5. Magnetization loop for TP 316L, cycled up to different usage factors  $D$ .

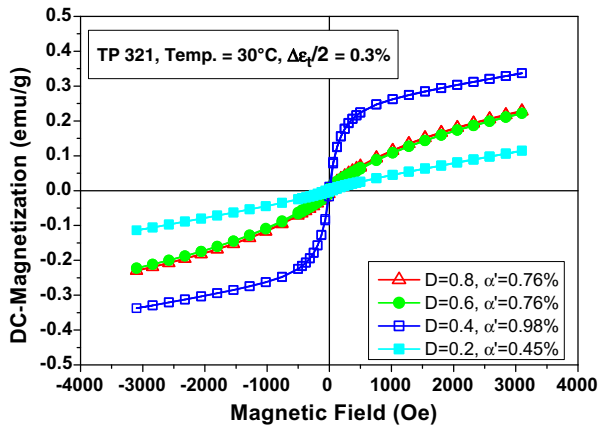


Fig. 6. Magnetization loop for TP 321, cycled up to different usage factors  $D$ .

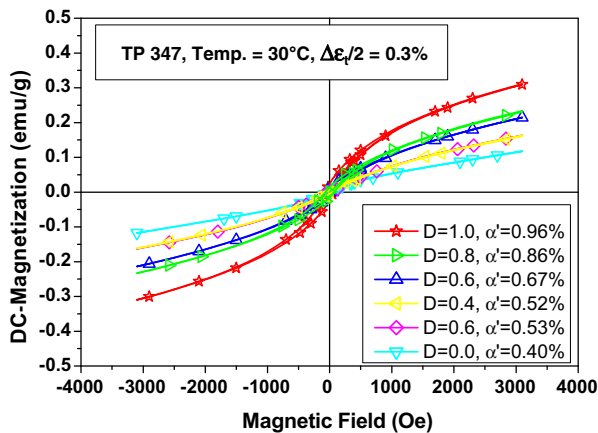


Fig. 7. Magnetization loop for TP 347, cycled up to different usage factors  $D$ .

Figs. 4–7 show the influence of the  $\alpha'$ -content on the shape of the magnetization loops. The virgin material ( $D = 0$ , Figs. 4–7) with low  $\alpha'$ -content shows almost paramagnetic behaviour, whereas the fatigued material becomes ferromagnetic, as can be observed from the S-shaped magnetization curve. However, for material TP 316L and TP 304L the magnetization is much smaller than in the other materials. The reason for this low  $\alpha'$ -formation in these unstabilized materials is the higher stability of the austenite phase than in the stabilized materials. Since in the investigated materials the energy dissipation during a magnetization loop is very small (in contrast to that shown for AISI 321 in Fig. 3), the hysteresis curve appears as a single line in the figures.

### 5. AC-magnetization loops of TP 321, 347, 304L and TP 316L

In the AC-mode, a small alternating magnetic field, a so-called minor loop, with the amplitude of 10 Oe (796 A/m) and a frequency of 1 kHz and 10 kHz, respectively, is superimposed to an applied DC-field. This method yields the field dependent permeability, a property very sensitive to small amount of ferritic contents in a paramagnetic matrix. For more detailed description of the method we refer to [14]. AC-measurements were performed in the range from  $H = -3000$  Oe to  $+3000$  Oe. The magnetization induced by the minor loops is given (again in emu/g) as a function of the magnetic field  $H$ .

The results of the AC-measurements are shown in Figs. 8–11. A high sensitivity of the AC-magnetization  $M_{AC}$  due to the  $\alpha'$ -content

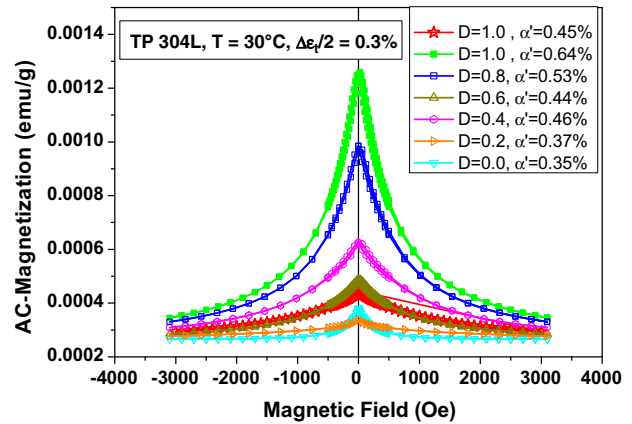


Fig. 8. AC-magnetization vs. magnetic field  $H$  for TP 304L, cycled up to different usage factors  $D$ .

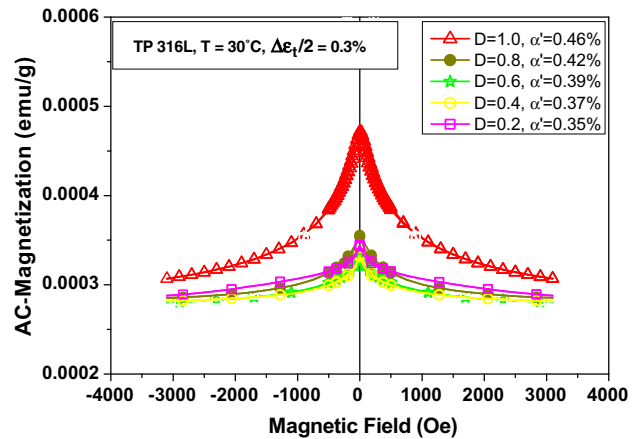


Fig. 9. AC-magnetization vs. magnetic field  $H$  for TP 316L, cycled up to different usage factors  $D$ .

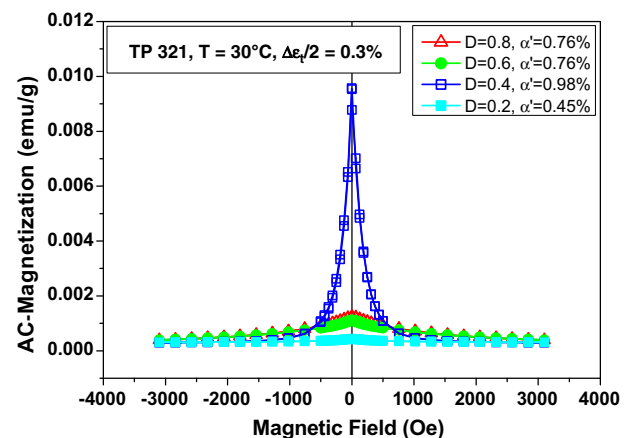


Fig. 10. AC-magnetization vs. magnetic field  $H$  for TP 321, cycled up to different usage factors  $D$ .

is shown for the investigated materials. Obviously, the sensitivity is highest at zero applied field ( $H = 0$ ). The relative change of this peak value is shown in Table 2. As expected, the smallest AC-magnetization was observed for un-stabilized steels TP 316L and TP 304L.

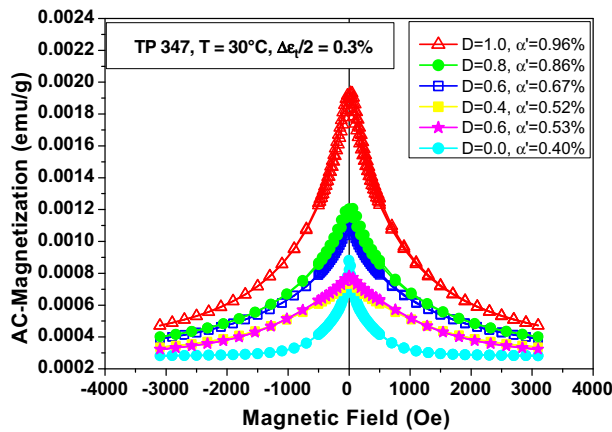


Fig. 11. AC-magnetization vs. magnetic field  $H$  for TP 347, cycled up to different usage factors  $D$ .

### 6. Sensitivity of magnetic parameters of TP 321, 347, 304L and TP 316L

Several magnetic parameters can be evaluated from the magnetization loops. Among these are the saturation magnetization  $M_s$ , remanent magnetization  $M_R$ , coercive field  $M_C$ , field dependent permeability and integrated hysteresis loop  $I_{M_{DC}}$ . The value  $I_{M_{DC}}$  corresponds to the energy dissipation (hysteresis heat) represented by the area within one hysteresis loop [15]. All these magnetic parameters are sensitive to the martensite content which itself is well correlated to the accumulated plastic strain of the specific material as shown for TP 304L in Fig. 2.

In Table 2 the sensitivities of the magnetic parameters vs. the amount of  $\alpha'$  are given within the range of  $0 < \alpha' < 3\%$ , corresponding to usage factors in the range  $0 \leq D \leq 1$ . The sensitivity is given as relative changes in vol.% of the magnetic parameters. It was observed that even though the increase of martensite is below 1%, the change of the concerning magnetic parameters is significant. As shown in Table 2, all the magnetic parameters are increased due to fatigue. The most sensitive parameters evaluated by analysing the magnetization loop are the integral  $I_{M_{DC}}$  and the peak value  $I_{M_{DC}}$  of the AC-magnetization. Even if the relative change of  $M_{DC3000}$  determined for TP 316L is only 1%, the corresponding relative change of  $M_{AC}$  is still about 36%. This in fact demonstrates the advantage of applying minor loops.

### 7. Influence of operating temperature on the magnetization curves

In Figs. 12 and 13 we compare the magnetization ( $M_{DC}$  and  $M_{AC}$ ) of material TP 321 for the operating temperatures, this is the temperature at which the material was fatigued,  $T = 80^\circ\text{C}$  and

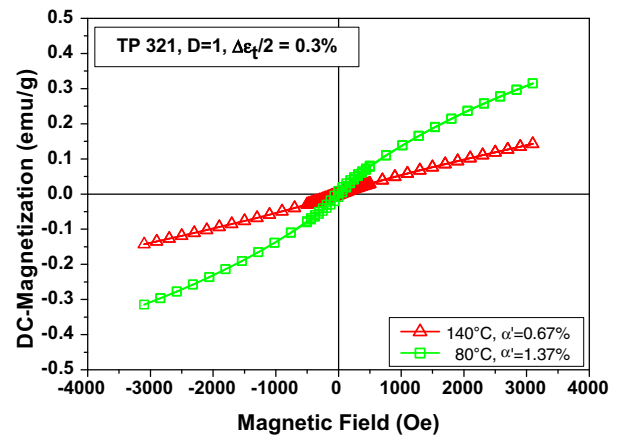


Fig. 12. DC-magnetization vs. magnetic field  $H$  for TP 321, operating temperatures  $80^\circ\text{C}$  and  $140^\circ\text{C}$ , respectively.

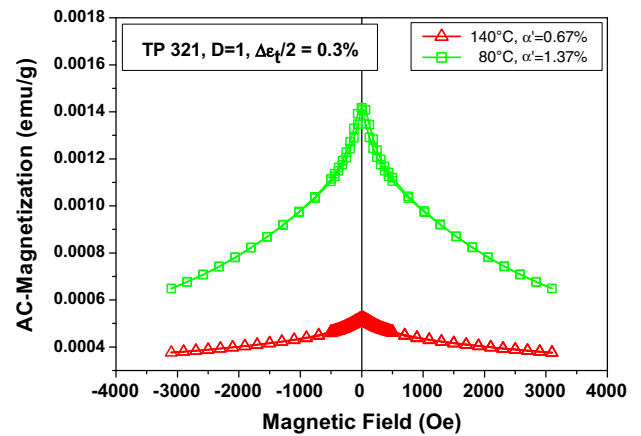


Fig. 13. AC-magnetization vs. magnetic field  $H$  for TP 321, operating temperatures  $80^\circ\text{C}$  and  $140^\circ\text{C}$ , respectively.

$T = 140^\circ\text{C}$ , respectively. Notice, that fatiguing the samples either at  $T = 80^\circ\text{C}$  or  $T = 140^\circ\text{C}$ , leads to an absolute difference  $\Delta\alpha'$  of only about 0.7% [4]. Nevertheless, the difference between the formed  $\alpha'$  at  $T = 80^\circ\text{C}$  and  $T = 140^\circ\text{C}$  results in a huge change of the corresponding magnetization curves. This difference is pronounced in the  $M_{AC}$  curve.

### 8. Discussion

In general the results of DC and AC measurements of the magnetization loops are in agreement and both kind of measurements

Table 2

Relative changes of the remanent magnetization  $M_R$ , coercive field  $M_C$ , DC-magnetization at  $\pm 3000$  Oe  $M_{DC3000}$ , hysteresis heat  $I_{M_{DC}}$  and peak value of the AC-magnetization  $M_{AC}$  due to fatigue of ASS

Parameters influencing the magnetic properties				Relative change in % of					
Material		$\alpha'$ in vol.%	$D$	$N$	$M_R$	$M_C$	$M_{DC3000}$	Integral $I_{M_{DC}}$	Peak $M_{AC}$
TP 304L	from	0.37	0.2	6332	1055	109	105	995	274
	to	0.64	1	38614					
TP 316L	from	0.35	0.2	7188	88	33.3	1	244	36
	to	0.46	1	46942					
TP 321	from	0.45	0.2	4679	116		177	189	228
	to	0.1.37	1	26890					
TP 347	from	0.41	0	0	518	181	446	745	104
	to	0.96	1	51710					

The influencing parameters are the content of martensite  $\alpha'$ , usage factor  $D$  and the number of strain cycles  $N$ .

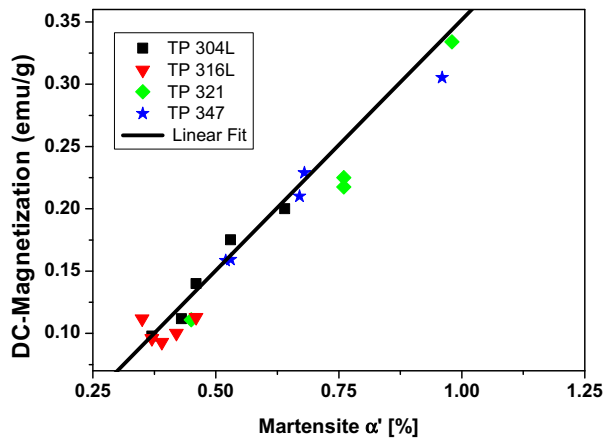


Fig. 14. DC-magnetization  $M_{3000}$  of different ASS in an external field of 3000 Oe.

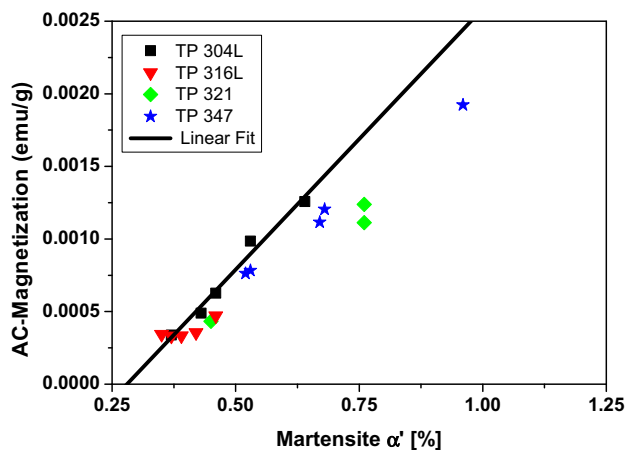


Fig. 15. AC-magnetization at external field  $H = 0$  of different ASS in an AC-field of 10 Oe.

allow to clearly distinguish between material with different martensite contents. Excellent correlation between the amount of  $\alpha'$  formed and the magnetic properties was observed. However, in a few cases the values of the magnetic properties do not seem to correspond well with the usage factor  $D$  as shown in Fig. 6 for TP 321, where more  $\alpha'$  was formed for  $D = 0.4$  than for  $D = 0.6$ . This is a consequence of the inhomogeneity of this material and the low affinity for  $\alpha'$ -formation. It is also worth mentioning that the usage factor  $D$  is somewhat artificial, since  $D = 1$  was determined from the average of a few samples and certainly differs from that of a particular specimen. It has also to be kept in mind that the measurement of the  $\alpha'$ -content was made within an uncertainty of about  $\pm 0.1\%$ .

Figs. 14 and 15, finally summarizes the results for the DC and AC measurements of all TP materials. Again we stress that each curve corresponds to a special sample taken from different locations of the tube. The linear increase of the magnetization as a function of the  $\alpha'$ -content is clearly demonstrated. It also turned out that the magnetization is only slightly dependent on the material but mainly dependent on the amount of  $\alpha'$ .

## 9. Conclusions

Since the martensite formation occurs parallel to the fatigue damage evolution, measuring the increase of  $\alpha'$  by appropriate methods in principle allows determining the fatigue state. How-

ever, for austenitic stainless steels with a low affinity for strain induced  $\alpha'$ -transformation, present measuring techniques have to be enhanced or supplemented by other principles. The aim of the presented investigations was to evaluate sensitive magnetic parameters, suitable to determine the fatigue state of the austenitic stainless steels with very low affinity for strain-induced martensite formation. Isothermal fatigue experiments and subsequent determination of the amount of martensite by neutron diffraction and magnetic measurements have shown the small sensitivity for strain-induced martensite formation in the investigated tube and pipe materials.

Measuring the whole magnetization loop of the fatigued austenitic stainless steels TP 321, 347, 304L and 316L yields several magnetic parameters, all of them being very sensitive to the amount of strain induced martensite. Among the evaluated parameters the integral  $MdH$  over the hysteresis loop and the magnetization induced by the minor loops of small amplitude appeared to be the most sensitive indicators for the amount of strain induced martensite, i.e. to the degree of fatigue.

We therefore conclude that applying magnetic minor loops is promising for the non-destructive evaluation of fatigue in austenitic stainless steels, especially in cases where very small amounts of strain-induced martensite are formed. The realisation and application of NDT-techniques utilising minor loops is therefore recommended.

## Acknowledgments

The financial support for this work by the Swiss Federal Nuclear Inspectorate (HSK) is gratefully acknowledged. We thank Dr M. Schneider and Dr P. Allenspach from the Laboratory for Neutron Scattering for their assistance on the PPMS. Furthermore we thank M. Stricker for the sample preparation and his help with the magnetic measurements.

## References

- [1] G.B. Olsen, M. Cohen, Kinetics of strain induced martensite nucleation, Metall. Trans. 6A (1975) 791–795.
- [2] D. Hennesy, G. Steckel, C. Alstetter, Phase transformation of stainless steel during fatigue, Metal. Trans. A. 7A (1977) 415.
- [3] G. Baudry, A. Pineau, Influence of strain-induced martensitic transformation on the low cycle fatigue behaviour of stainless steel, Mater. Sci. Eng. 28 (1977) 229.
- [4] M. Niffenegger, D. Kalkhof, H.J. Leber, Determination of deformation-induced Martensite in austenitic stainless steel, in: Fourth International Conference on NDT in Relation to Structural Integrity for Nuclear and Pressurised Components, London, JRC/EPRI, 2004.
- [5] D. Kalkhof, M. Grosse, M. Niffenegger, H. Leber, Monitoring fatigue degradation in austenitic stainless steels, Fatigue Fract. Eng. Mater. Struct. 27 (2004) 595.
- [6] B. Acosta et al. Project GRETE: Evaluation of Non-Destructive Testing Techniques for Monitoring of Material Degradation, NDT-net, August 2002, vol. 7, No. 08.
- [7] G. Dobmann, et al., Non-destructive Characterization of Early Fatigue Damage in Austenitic Stainless Steels by use of Micro Magnetic Methods, in: Proceedings of the Third International Conference on Fatigue of Reactor Components, OECD NEA CSNI, Paris, France, 2004.
- [8] F. Förster, Über Fortschritte der zerstörungsfreien Materialprüfung mit elektromagnetischen Verfahren, Materialprüfung 4 (1962) 397.
- [9] M.A. Lang, Non-destructive evaluation of deformation-induced martensite formation of austenitic steel X6CrNiTi18-10 by means of high sensitive magnetometers, Dissertation, University of Saarbrücken, Germany, 2000.
- [10] V. Schoss, Martensitische Umwandlung und Ermüdung austenitischer Edelmetalle, Gefügeveränderungen und Möglichkeiten der Früherkennung von Ermüdungsschädigungen, Dissertation, Technische Universität Bergakademie Freiberg, 2001.
- [11] M. Grosse, M. Niffenegger, D. Kalkhof, Monitoring of low-cycle fatigue degradation in X6CrNiTi18-10 austenitic steel, J. Nucl. Mater. 296 (2001) 305.
- [12] T. Liu et al., Stray flux effects on the magnetic hysteresis parameters in NDE of low carbon steel, NDT&E Int. 39 (2006) 277.
- [13] K. Mumtaz et al., Detection of martensite transformation in high temperature compressively deformed austenitic stainless steel by magnetic NDE technique, J. Mater. Sci. 38 (2003) 3037.
- [14] <<http://www.qdusa.com>>.
- [15] E. Warburg, Ann. Phys. Lpz. 13 (1881) 141.